Supporting Information

Continuous detection of HCl and NH_3 gases with a high-performance fluorescent polymer sensor

Ning Xu,[a] Rui-Lei Wang,[a] Dong-Peng Li,[a] Zi-Yan Zhou,[a]* Tian Zhang,[a]* Yu-Zhong Xie,[b]* Zhong-Min Su[c]

[a]*School of Chemistry and Chemical Engineering, Shandong University of Technology, Zibo 255000, People's Republic of China.*

[b]*Department of Chemistry, Yanbian University, Yanji 133002, People's Republic of China.*

[c]*Institute of Functional Material Chemistry, Faculty of Chemistry, Northeast Normal University, Changchun 130024, People's Republic of China*

*Corresponding authors.

E-mail addresses: zyzhou@sdut.edu.cn (Z.-Y. Zhou); tzhang@sdut.edu.cn (T. Zhang); whyjs@ybu.edu.cn (Y. -Z. Xie)

Table S1 Yields of COP-1 synthesized under different reaction conditions

Entry	Raw material ratios (2, 4, 6-trimethyl-1, 3, 5-triazine : 1, 4-Phthalaldehyde)	Temperature (℃)	Yield (%)
1	1 : 1	70	72
2	2 : 3	70	69
3	1 : 2	70	56
4	1 : 1	80	62
5	2 : 3	80	78
6	1 : 2	80	58
7	1 : 1	90	74
8	2 : 3	90	75
9	1 : 2	90	57

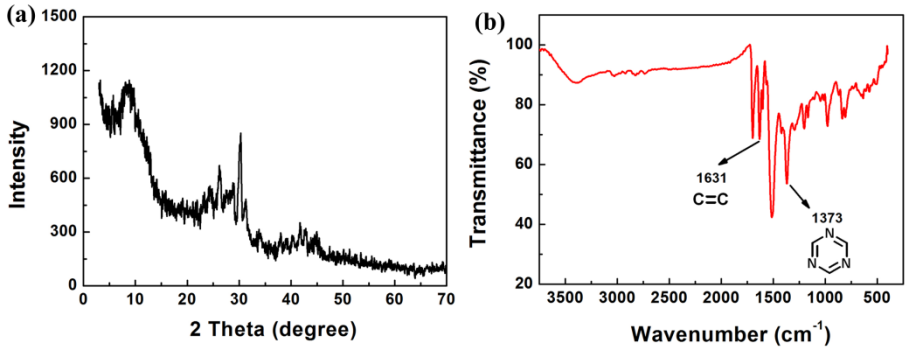

Fig. S1. Powder XRD pattern (a) and FT-IR spectrum (b) of **COP-1**.

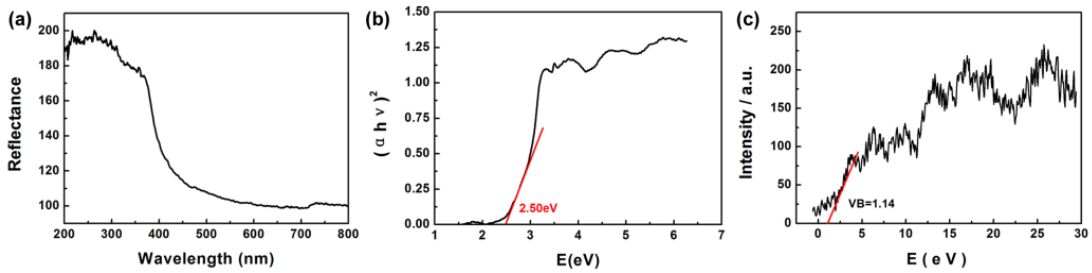

Fig. S2. UV-Vis DRS (a), $(\alpha h\nu)^2$ versus ($h\nu$) curve obtained from (a) to examine the energy gap (b) and VB-XPS (c) of **COP-1**

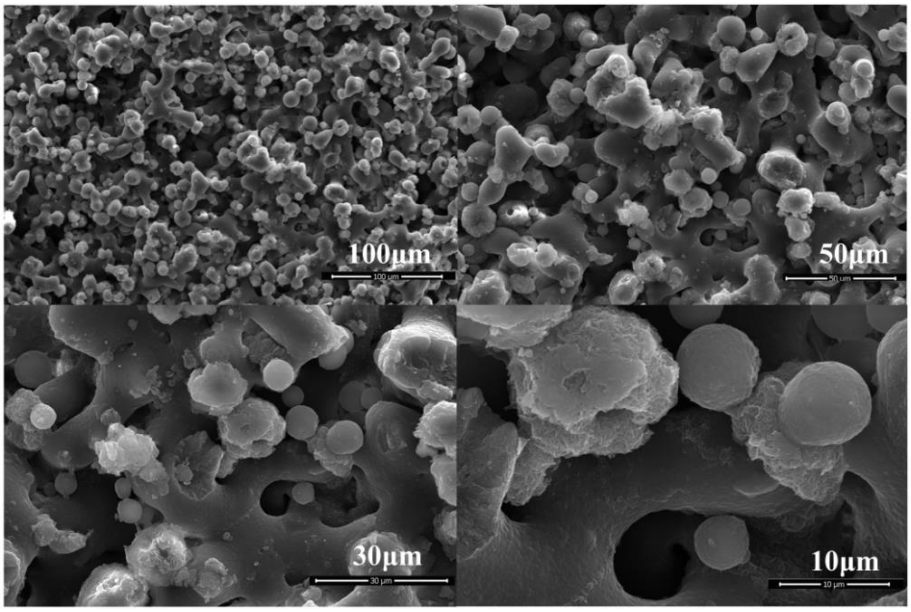

Fig. S3. SEM images of the **COP-1** film.

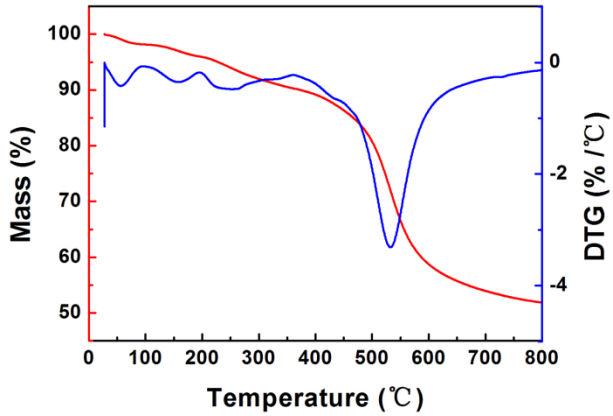

Fig. S4. TG (in red line) and DTG (in blue line) curves of **COP-1**.

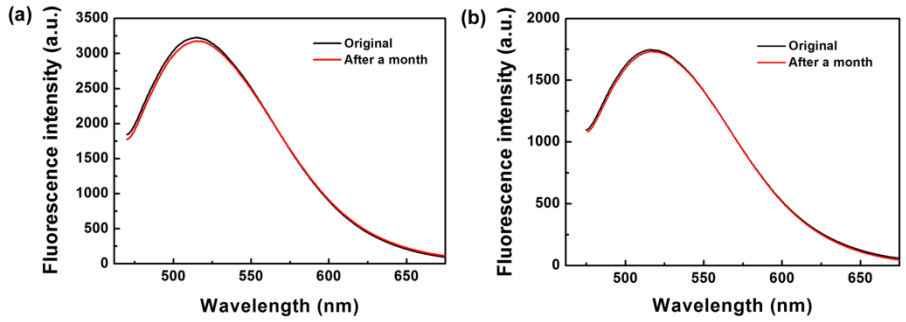

Fig. S5. Fluorescence spectra of the **COP-1** powders (a) and **COP-1** film (b) before and after a month.

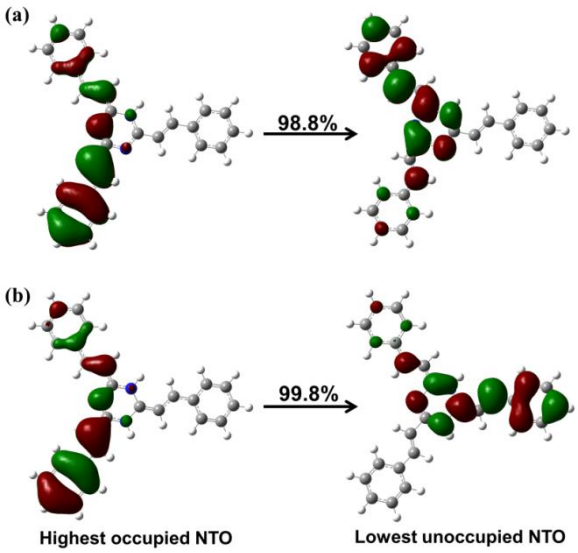

Fig. S6. NTO character and transition proportion of the S_1 states for COM-1-1P (*a*) and COM-1-2P (*b*).

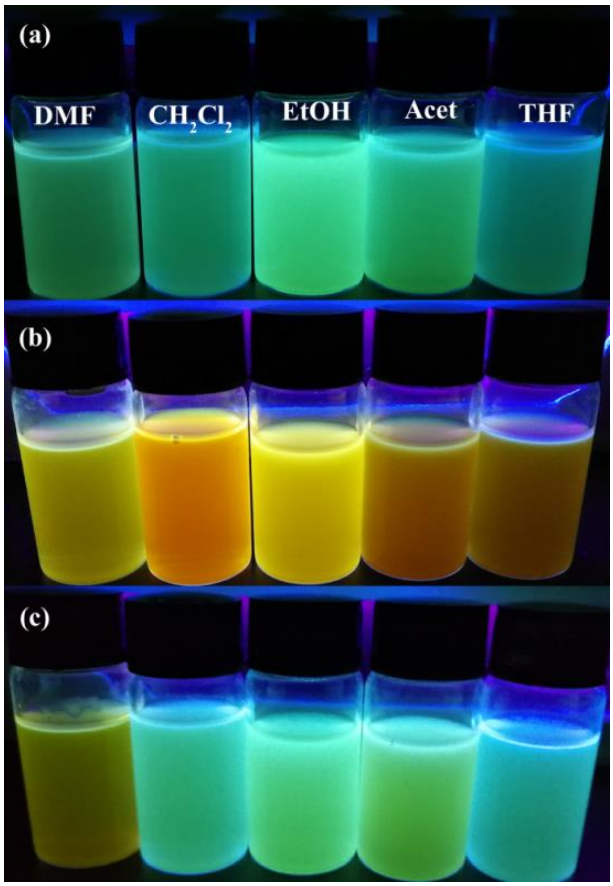

Fig. S7. (a) Fluorescence of the **COP-1** powders dispersed in different solvents; (b) Fluorescence of the **COP-1** powders dispersed in different HCl-bubbled solvents; (c) Fluorescence of the **COP-1** powders in (b) via subsequent injection with NH_3.

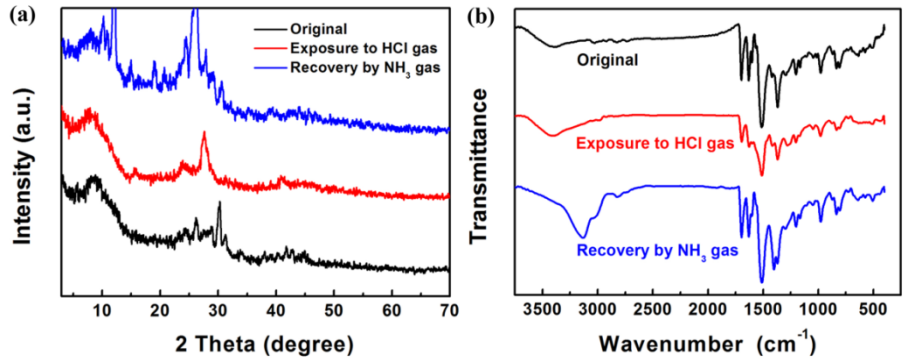

Fig. S8. Powder XRD patterns (a) and FT-IR spectra (b) of the **COP-1** powders before and after exposed to HCl gas, and recovery by NH_3 gas.

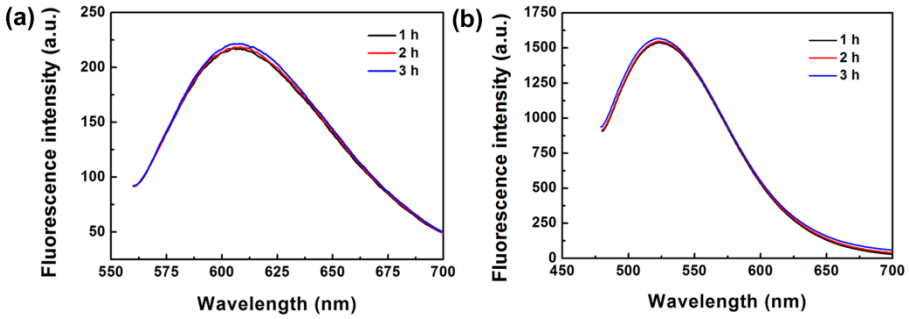

Fig. S9. Fluorescence stability of the **COP-1** film for detection of HCl gas (a) and NH_3 gas (b).

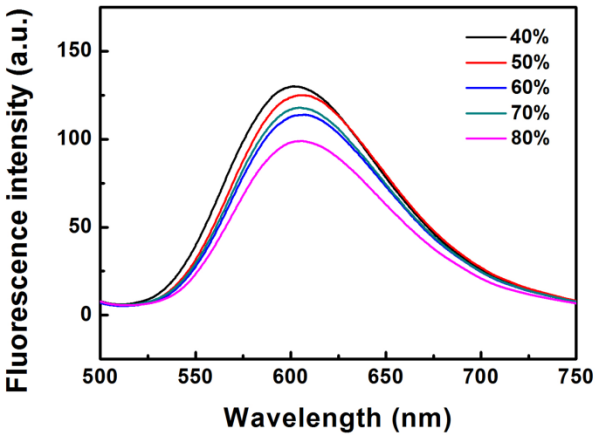

Fig. S10. Detection of HCl gas under different humidity environments (40%, 50%, 60%, 70% and 80%) by COP-1.